

On the analysis of jointed Euler-Bernoulli beams with step changes in material and cross-section under static and dynamic loads

Filippo Giunta^{1,2}, Alice Cicirello^{2*}

¹ Department of Engineering, University of Messina, Villaggio S. Agata, 98166 Messina, IT

² Department of Engineering Science, University of Oxford Parks Road, Oxford OX1 3PJ, UK

Emails: fgiunta@unime.it, alice.cicirello@eng.ox.ac.uk

Abstract

Many engineering systems can be modelled as an assembly of beams with different material properties and cross-sections jointed at their edges. This paper presents an approach to analyse jointed Euler-Bernoulli (EB) beams with step changes in material and cross-section under static and dynamic loads. The standard approaches to tackle this type of problem are not completely satisfactory in terms of: (i) computational efficiency in dealing with step changes in material and cross-section, when the continuity conditions must be enforced with auxiliary equations (classic approach) or when a denser mesh has to be used at the discontinuity interfaces (Finite Element Method); (ii) taking into account efficiently internal and external springs at the discontinuity interfaces; (iii) numerical errors in the evaluation of high-order modes for jointed beams. An approach is proposed to overcome these limitations. This approach tackles an assembly of n piecewise homogenous EB beams jointed at their edges using the generalized functions to obtain a single expression of the solution which depends on the 4 integration constants associated with the boundary conditions. Closed-form expressions of the 4 constants are provided. Further, in the presence of internal or external springs, additional constants representing the discontinuities have to be taken into account. The latter are computed by considering one additional condition for each discontinuity. The proposed approach is particularized for the static and dynamic analysis (modal analysis and forced vibration analysis). The feasibility of the proposed approach is shown with two numerical applications.

1. Introduction

Robot arms, drill strings, pipelines, and helicopter rotor blades are examples of engineering systems which can be modelled as beam-like elements with different material properties and cross sections jointed at their edges. The analysis of jointed Euler-Bernoulli (EB) with step changes in material and cross-section under static and dynamic loads can be performed with the classic method. Considering, an assembly of n EB beams jointed at their edges the classical method is based on writing a set of n governing equations and impose the $4(n-1)$ continuity conditions (one for each interface). Therefore, this approach requires the evaluation of the $4(n-1)$ integration constant, so as a result it can be time-consuming as the number of EB beams increases. Another standard approach for tackling this type of problems is to use the Finite Element Method (FEM). Similarly, this may require significant inputs from the user in the modelling phase. Moreover, the accuracy of the results will depend on the density of the mesh. A denser mesh is required at the interfaces and as known, the denser is the mesh, the more computational effort is required. Thus, this approach becomes time consuming for complex built-up beams system. Furthermore, the above-mentioned approaches cannot be easily used for exploring the performance of different designs, and numerical errors in the evaluation of high-order modes may occur.

Alternative and more efficient procedures for evaluating the static response of EB beams with mechanical or geometrical discontinuities have been developed in recent years. Yavary et al. [2000,2001], tackled the static case problem of jointed EB beams with different material properties and cross sections (flexural rigidity) with internal rotational springs (slope discontinuity) and translational springs (displacement discontinuity) by proposing the so-called auxiliary-beam method. This approach requires enforcing 4 boundary conditions and $2N$ continuity conditions if the three kinds of discontinuities are present simultaneously. If only the flexural rigidity discontinuity is present, the method still requires the enforcement of $2N$ continuity conditions in addition to the boundary conditions. An alternative procedure for the static case has been developed by Biondi and Caddemi [2005,2007], who provided a closed-form solution, dependent on boundary conditions only for the jointed EB beams with one or

multiple step changes in material proprieties and cross-sections with internal rotational springs by using the generalised functions.

The dynamic response of jointed EB beams has been tackled in literature by using various techniques. Koplow et al. [2006] provided an analytic solution for the mode shapes of jointed EB beam with a single step change in the material and cross-section by coupling two separate uniform EB beams and by imposing the continuity conditions using a matrix approach. Stanton and Mann [2010] generalized the method provided Koplow et al. [2006] to address multiple discontinuities. In both methods, the inversion of matrices is required. The previous methods take into account of the ideal joints only. Torabi et al. [2013] used the transfer matrix method to evaluate the free vibration response of jointed EB with step changes in cross-sections with ideal joints. Failla and Santini [2008] provided a closed-form solution for the free vibration response of jointed EB beams with internal translational and rotational springs by using a lumped-mass approximation and employing exact influence coefficients by defining some ad-hoc Green's functions. This approximate method is computationally efficient to solve the eigenvalue problem. Recently, Lin and Ng [2017] presented an approach for the vibration analysis of jointed EB with step changes in cross-section with translational springs and rotational springs at the interfaces, using the elemental impedance method.

It is worth noting that the assessment of the natural frequencies (and related mode shapes) of a beam can be affected by numerical instabilities due to the presence of the hyperbolic functions in the closed-form solution of the free vibrations, to the point of being able to accurately compute only up to 12 modes depending on the boundary conditions [Gonçalves et al. 2007]. These numerical instabilities can become significant for stepped beams as reported by Xu et al [2013] limiting the number of modes that can be accurately computed. Xu et al [2013] tackled the free vibration analysis of jointed EB with step changes in material proprieties and cross sections with ideal joints by writing the governing equations of each segment of the stepped beam in its local coordinate system and by coupling them with continuity conditions at the interface points. The local coordinate system simplifies the expression of the frequency determinant (characteristic equation) of the stepped beam, which leads to a large elimination of numerical round-off errors and consequently improving the accuracy on the evaluation of the high-order mode shapes.

In this paper, an efficient approach is presented for the analysis of jointed EB beams with step changes in material and cross-section with internal rotational springs, internal translational springs and external translational springs at the interfaces, under static (**Section 2**) and dynamic (**Section 3.2.1, Section 3.2.2**) loads. In particular, the generalized functions are used to obtain a single expression of the solution (in terms of deflection or mode shapes) which depends on the 4 integration constants associated with the boundary conditions, and closed-form expression of these 4 integration constants are provided. One additional constant is required for each internal or external spring at the interfaces, which can be computed by also enforcing one additional condition. Similarly to the approach suggested by Xu et al [2013] for the dynamic analysis of stepped beams, the numerical instabilities due to the hyperbolic functions for computing higher order modes have been reduced by writing the governing equation of each segment in its local coordinate system. The feasibility of the proposed approach is shown with two numerical applications, on the static (**Section 4.1**) and dynamic (**Section 4.2**) analysis of EB beams with step changes in material and cross-sections with general boundary conditions, internal rotational, internal translational and external translational springs at the interfaces. Moreover, the accuracy of the results provided by the proposed approach is assessed by direct comparison with the results yielded by the commercial FEM software CSI Sap2000®.

2. Closed-form solution for the static analysis of jointed Euler-Bernoulli beams

Let us consider an assembly of $N+1$ Euler-Bernoulli (EB) beams with uniform flexural stiffness, being N the number of discontinuity points, as shown in **Figure 1**.

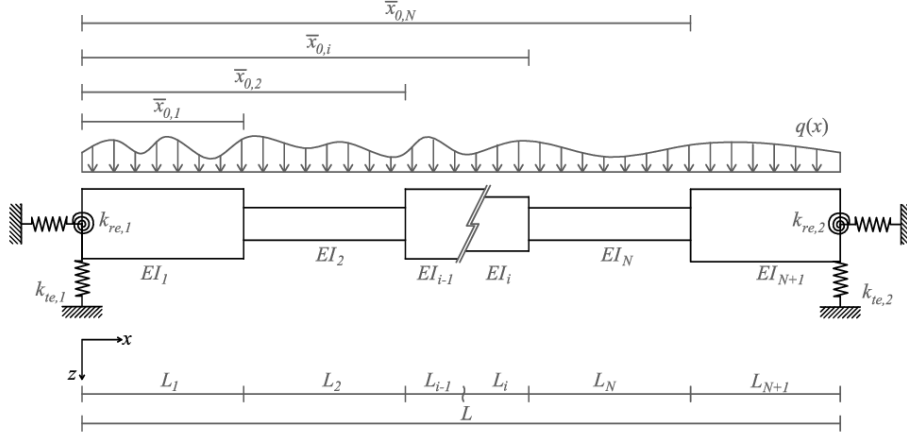


Figure 1 Euler-Bernoulli beam with multiple step changes in cross-section and arbitrary boundary conditions subjected to an arbitrary static load.

Where $k_{te,1}$, $k_{te,2}$, and $k_{re,1}$, $k_{re,2}$ are respectively the translational and rotational stiffnesses, related to the boundary conditions of the jointed beam.

The differential equation governing the bending deflection of a EB beam with abscissa dependent flexural stiffness is:

$$\left[E(x)I(x)W''(x) \right]'' = q(x) \quad (1)$$

where x is the spatial coordinate spanning from 0 to the length L of the beam, $W(x)$ is the deflection and $q(x)$ is the transversal load acting on the beam (both positive if downward), and $E(x)I(x)$ is the flexural rigidity obtained by the product of the Young's modulus ($E(x)$) and the second moment of area ($I(x)$). The apex indicates differentiation with respect to x . The following kinematics and compatibility equations hold:

$$\Psi(x) = W'(x) \quad (2)$$

$$\chi(x) = W''(x) \quad (3)$$

$$M(x) = -E(x)I(x)W''(x) \quad (4)$$

$$T(x) = -(E(x)I(x)W''(x))' \quad (5)$$

Where $\Psi(x)$ and $\chi(x)$ are the slope and the curvature functions, respectively, while $M(x)$ and $T(x)$ are the bending moment and the shear force, respectively.

The generalized functions can be used to account efficiently for the step changes in the flexural rigidity, so that the flexural rigidity function can be written as:

$$EI(x) = EI_1 + \sum_{i=2}^{N+1} [EI_i(x) - EI_{i-1}(x)] H(x - \bar{x}_{0,i-1}) \quad (6)$$

Where $\bar{x}_{0,i}$ is the position of the discontinuity with respect to the global reference system, as indicated in **Figure 1**, $EI_i(x)$ is the flexural rigidity of the uniform i th EB beam, and $H(x - \bar{x}_{0,i-1})$ is the Heaviside's unit step function defined as:

$$H(x - \bar{x}_{0,i-1}) = \delta^{[1]}(x - \bar{x}_{0,i-1}) = \int_{-\infty}^{+\infty} \delta(x - \bar{x}_{0,i-1}) dx = \begin{cases} 0, & x < \bar{x}_{0,i-1} \\ \frac{1}{2}, & x = \bar{x}_{0,i-1} \\ 1, & x > \bar{x}_{0,i-1} \end{cases} \quad (7)$$

being $\delta(x - \bar{x}_{0,i-1})$ the Dirac's delta function and $\delta^{[1]}(x - \bar{x}_{0,i-1})$ its primitive.

Since we are dealing with a linear problem, the superposition principle holds. Therefore, the deflection $W(x)$ of the EB jointed beam can be expressed as:

$$W(x) = W_1(x) + \sum_{i=2}^{N+1} [W_i(x) - W_{i-1}(x)] H(x - \bar{x}_{0,i-1}) \quad (8)$$

Being $W_i(x)$ the deflection of an equivalent homogeneous beam with flexural rigidity corresponding to EI_i , which can be obtained using the standard approach:

$$W_i(x) = \frac{Q^{[4]}(x)}{EI_i} + \frac{C_{1,i}}{6} x^3 + \frac{C_{2,i}}{2} x^2 + C_{3,i} x + C_{4,i} \quad (9)$$

where $Q^{[k]}$ is a function evaluated as a primitive of the order k of the external load function $q(x)$, while, $C_{1,i}$, $C_{2,i}$, $C_{3,i}$ and $C_{4,i}$ are the $4N$ unknowns coefficients dependent on the continuity and boundary conditions. It is worth noting that the transversal load $q(x)$ can be expressed with the generalised functions, so that for example a point force of amplitude F_0 applied at abscissa x_F can be written as $q(x) = F_0 \delta(x - x_F)$.

Dimensionless quantities can be introduced to describe the relationships between the flexural rigidities of two successive segments:

$$\tilde{\gamma}_i = \frac{EI_{i+1}}{EI_i} \quad (10)$$

These quantities, together with the enforcement of the continuity conditions in terms of displacement ($W_i(\bar{x}_{0,i}) = W_{i+1}(\bar{x}_{0,i})$), rotation ($\Psi_i(\bar{x}_{0,i}) = \Psi_{i+1}(\bar{x}_{0,i})$), shear force ($T_i(\bar{x}_{0,i}) = T_{i+1}(\bar{x}_{0,i})$) and bending moment ($M_i(\bar{x}_{0,i}) = M_{i+1}(\bar{x}_{0,i})$), enable to reduce the $4N$ unknown coefficients to 4 unknown coefficients which depend on the boundary conditions only:

$$C_{1,i+1} = \frac{C_{1,i}}{\tilde{\gamma}_i} \quad (11)$$

$$C_{2,i+1} = \frac{C_{2,i}}{\tilde{\gamma}_i} \quad (12)$$

$$C_{3,i+1} = -\frac{1}{2EI_i \tilde{\gamma}_i} \left\{ EI_i \left[-2C_{3,i} \tilde{\gamma}_i + (C_{1,i} \bar{x}_{0,i}^2 + 2C_{2,i} \bar{x}_{0,i})(1 - \tilde{\gamma}_i) \right] + 2Q^{[3]}(\bar{x}_{0,i})(1 - \tilde{\gamma}_i) \right\} \quad (13)$$

$$C_{4,i+1} = -\frac{1}{6EI_i \tilde{\gamma}_i} \left[EI_i \left\{ -\bar{x}_{0,i}^2 (3C_{2,i} + 2C_{1,i} \bar{x}_{0,i}) + \tilde{\gamma}_i \left[-6C_{4,i} + \bar{x}_{0,i}^2 (3C_{2,i} + 2C_{1,i} \bar{x}_{0,i}) \right] \right\} \right. \\ \left. + 6(Q^{[4]}(\bar{x}_{0,i}) - \bar{x}_{0,i} Q^{[3]}(\bar{x}_{0,i}))(1 - \tilde{\gamma}_i) \right] \quad (14)$$

These expressions (Eqs. (11), (12), (13), (14)) can be directly used in Eq. (9), and therefore in Eq. (8). Eq. (8) is consequently a function of only $C_{1,1}$, $C_{2,1}$, $C_{3,1}$ and $C_{4,1}$. By imposing the boundary conditions (two conditions at $x=0$ and two others at $x=L$) to the general expression in Eq. (8), these 4 constants can be evaluated.

In a similar fashion $\Psi(x)$, $M(x)$ and $T(x)$ functions can be expressed as:

$$\Psi(x) = \Psi_1(x) + \sum_{i=2}^{N+1} [\Psi_i(x) - \Psi_{i-1}(x)] H(x - \bar{x}_{0,i-1}) \quad (15)$$

$$M(x) = M_1(x) + \sum_{i=2}^{N+1} [M_i(x) - M_{i-1}(x)] H(x - \bar{x}_{0,i-1}) \quad (16)$$

$$T(x) = T_1(x) + \sum_{i=2}^{N+1} [T_i(x) - T_{i-1}(x)] H(x - \bar{x}_{0,i-1}) \quad (17)$$

where:

$$\Psi_i(x) = \frac{Q^{[3]}(x)}{EI_i} + \frac{C_{1,i}}{2} x^2 + C_{2,i} x + C_{3,i} \quad (18)$$

$$M_i(x) = -EI_i \left(\frac{Q^{[2]}(x)}{EI_i} + C_{1,i} x + C_{2,i} \right) \quad (19)$$

$$T_i(x) = -EI_i \left(\frac{Q^{[1]}(x)}{EI_i} + C_{1,i} \right) \quad (20)$$

The presence of internal rotational and translational springs, and along-axis external springs at interface points can now be taken into account by using the generalised functions to convert the discontinuities into terms of a generalised load function.

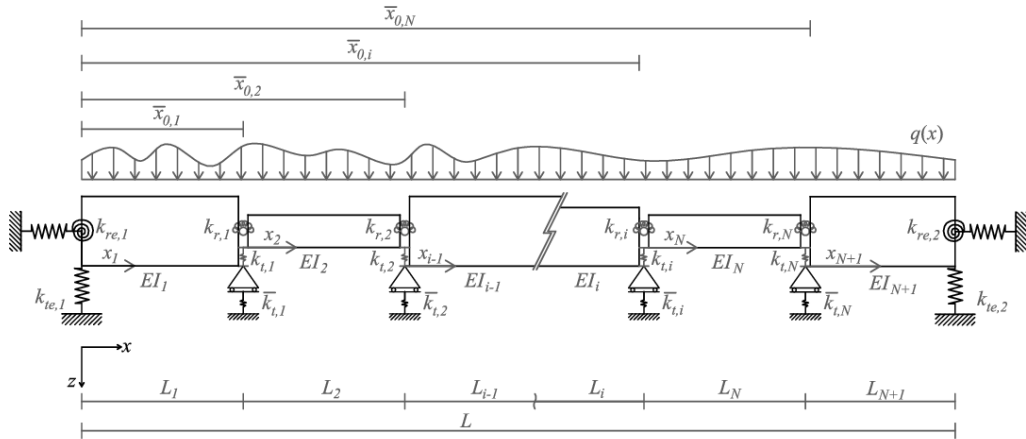


Figure 2 Jointed EB beam with multiple step changes in cross-section, arbitrary boundary conditions, along-axis springs and internal rotational and translational springs at the discontinuities, subjected to an arbitrary static load.

Let us consider the case where external translational, internal rotational and internal translational springs are located at each discontinuity point as shown in **Figure 2**. The generalised load function $\bar{q}(x)$ can be written as follow:

$$\bar{q}(x) = q(x) + \sum_{i=1}^N \Delta T_i \delta(x - \bar{x}_{0,i}) + \sum_{i=1}^N EI_i \Delta \psi_i \delta''(x - \bar{x}_{0,i}) + \sum_{i=1}^N EI_i \Delta w_i \delta''(x - \bar{x}_{0,i}) \quad (21)$$

where $q(x)$ is the static load distribution, $\Delta T_i, \Delta \psi_i, \Delta w_i$ are the unknown variations of $T(\bar{x}_{0,i})$, $\Psi(\bar{x}_{0,i})$ and $W(\bar{x}_{0,i})$, respectively. Moreover, the terms $\delta''(x - \bar{x}_{0,i})$ and $\delta'''(x - \bar{x}_{0,i})$ are respectively the second and third derivative respect to the x of the Dirac's delta function. Each unknown variation is found by writing one additional condition. This means that for r unknown variations, the deflection of the beam is found by solving a set of $4+r$ equations, being 4 the number of boundary conditions.

The internal rotational springs (stiffness $k_{r,i}$), internal translational springs (stiffness $k_{t,i}$) and along-axis external translational springs (stiffness $\bar{k}_{t,i}$) at the discontinuity interfaces can be expressed as:

$$M(\bar{x}_{0,i}) = k_{r,i} \Delta \psi_i \quad (22)$$

$$T(\bar{x}_{0,i}) = k_{t,i} \Delta w_i \quad (23)$$

$$W(\bar{x}_{0,i}) = -\frac{\Delta T_i}{\bar{k}_{t,i}} \quad (24)$$

In summary, the proposed approach provides a closed-form solution for the static analysis of jointed EB beams. When only variations in the flexural rigidity occur, only 4 boundary conditions need to be enforced. One additional condition has to be enforced to take into account for each internal or along-axis external spring.

The proposed method is an efficient alternative to the auxiliary beam method proposed by Yavari et al. [2000], since it provides a closed-form solution for the static Euler-Bernoulli beams in presence of multiple flexural rigidity, slope and deflection jumps. The approach proposed by Yavari et al. [2000] requires imposing 2 continuity conditions for each change in the flexural rigidity, one for each internal rotational or translational spring. When all the three jumps occur at one location, only $2N$ continuity conditions are required. With the proposed method instead, no further conditions are required for flexural rigidity variations. When internal springs are present, the same number of conditions of [Yavari et al., 2000] are required. Finally, the proposed approach can also account for along-axis translational springs at the interface points. The proposed method is also an alternative to the one proposed by Biondi and Caddemi [2007]. Biondi and Caddemi provided a closed-form solution for the static analysis of EB beams in presence of multiple flexural-rigidity and slope discontinuities (in terms of rotational springs), which depends on the 4 boundary conditions only [Biondi and Caddemi, 2007]. This solution has been derived by using the product of two Dirac's deltas centred at the same point, therefore avoiding the need of an additional condition to be imposed at each slope discontinuity. However, internal translational connections or external support at the discontinuity interfaces were not investigated by the authors.

Moreover, the proposed formulation can be easily extended to tackle dynamic problems, as described in the following section.

3. Forced vibration analysis of jointed Euler-Bernoulli damped beams

Similarly to the static case, the jointed EB beam is considered as an assembly of $N+1$ EB beams, being N the number of discontinuity points. In **Section 3.1**, the standard procedure for the analysis of the forced vibration response of the generic i th EB damped beam is reviewed. **Section 3.2** will present the approach for the forced vibration analysis of the jointed EB damped beam.

3.1 Forced vibration analysis of the i th EB damped beam

The governing equation describing the response of the i th EB damped beam with uniform flexural rigidity EI_i , cross-section A_i and density ρ_i subjected to the dynamic transverse load $f_z(x_i, t)$ (being x_i the coordinate system such that $0 \leq x_i \leq L_i$ with L_i the length of the i th beam) is:

$$EI_i W_i''''(x_i, t) + c_{K,i} EI_i \dot{W}_i''''(x_i, t) + c_{M,i} \rho_i A_i \dot{W}_i(x_i, t) + \rho_i A_i \ddot{W}_i(x_i, t) = f_z(x_i, t) \quad (25)$$

where $W_i(x_i, t)$ is the time-dependent deflection of i th the beam, while $c_{K,i}$ and $c_{M,i}$ are the two constants of the Rayleigh damping model. The dot indicates differentiation with respect to time t , while the apex indicates the differentiation with respect to the abscissa x_i , so that $\dot{W}_i''''(x_i, t) = \partial \left[\partial^4 W_i(x_i, t) / \partial x_i^4 \right] / \partial t$, $\dot{W}(x, t) = \partial W(x, t) / \partial t$ is the velocity and $\ddot{W}(x, t) = \partial^2 W(x, t) / \partial t^2$ is the acceleration.

The time-dependent deflection $W_i(x_i, t)$ can be determined by using the mode superposition principle together with the method of separation of variables. Indeed, $W_i(x_i, t)$ can be assumed as the sum of the product of the s th mode shape $\hat{\Phi}_{i,s}(x_i)$, which depends on the spatial coordinate x_i and a time-dependent generalised coordinate in the s th mode $\mathcal{G}_{i,s}(t)$, as:

$$W_i(x_i, t) = \sum_{s=1}^{\infty} \hat{\Phi}_{i,s}(x_i) \mathcal{G}_{i,s}(t) \quad (26)$$

The undamped free vibrations are first considered, for which Eq. (25) becomes:

$$EI_i W_i''''(x_i, t) + \rho_i A_i \ddot{W}_i(x_i, t) = 0 \quad (27)$$

Replacing the Eq. (26) into Eq. (27), Eq. (27) can be written as:

$$EI_i \sum_{s=1}^{\infty} \hat{\Phi}_{i,s}''''(x_i) \mathcal{G}_{i,s}(t) + \rho_i A_i \sum_{s=1}^{\infty} \hat{\Phi}_{i,s}(x_i) \ddot{\mathcal{G}}_{i,s}(t) = 0 \quad (28)$$

Eq. (28), after simple manipulations, and considering only the p th mode shape, can be written as:

$$\frac{EI_i}{\rho_i A_i} \frac{\hat{\Phi}_{i,p}''''(x_i)}{\hat{\Phi}_{i,p}(x_i)} = - \frac{\ddot{\mathcal{G}}_{i,p}(t)}{\mathcal{G}_{i,p}(t)} = \omega_{i,p}^2 \quad (29)$$

Since the first member of the Eq. (29) is a function of x_i , and the second member is a function of t , both members have to be equal to the positive constant $\omega_{i,p}^2$, which is the square value of the natural frequency related to the p th mode shape.

Eq. (29) can be re-written as the two well-known equations:

$$\ddot{\mathcal{G}}_{i,p}(t) + \omega_{i,p}^2 \mathcal{G}_{i,p}(t) = 0 \quad (30)$$

$$\hat{\Phi}_{i,p}''''(x_i) - \eta_{i,p}^4 \hat{\Phi}_{i,p}(x_i) = 0 \quad (31)$$

where $\eta_{i,p}$ is the frequency parameter defined as:

$$\eta_{i,p} = \sqrt[4]{\frac{\rho_i A_i \omega_{i,p}^2}{EI_i}} \quad (32)$$

The solution of Eq. (30), can be expressed as a combination of trigonometric functions:

$$\mathcal{G}_{i,p}(t) = A_{i,p}^{(1)} \sin(\omega_{i,p} t) + A_{i,p}^{(2)} \cos(\omega_{i,p} t) \quad (33)$$

where the coefficients $A_{i,p}^{(1)}$ and $A_{i,p}^{(2)}$ are constants computed by imposing the two initial conditions: $W_i(x_i, t=0)$ and $\dot{W}_i(x_i, t=0)$.

The well-known solution of Eq. (31) is a combination of the trigonometric and hyperbolic functions:

$$\begin{aligned} \hat{\Phi}_{i,p}(x_i) = & \frac{C_{i,p}^{(1)}}{2} (\cos(\eta_{i,p} x_i) + \cosh(\eta_{i,p} x_i)) + \frac{C_{i,p}^{(2)}}{2\eta_{i,p}} (\sin(\eta_{i,p} x_i) + \sinh(\eta_{i,p} x_i)) - \\ & - \frac{C_{i,p}^{(3)}}{2\eta_{i,p}^2} (\cos(\eta_{i,p} x_i) - \cosh(\eta_{i,p} x_i)) - \frac{C_{i,p}^{(4)}}{2\eta_{i,p}^3} (\sin(\eta_{i,p} x_i) - \sinh(\eta_{i,p} x_i)) \end{aligned} \quad (34)$$

where, the coefficients $C_{i,p}^{(1)}, C_{i,p}^{(2)}, C_{i,p}^{(3)}, C_{i,p}^{(4)}$ are the 4 integration constants dependent on $\eta_{i,p}$, and which can be computed by imposing the 4 boundary conditions of the i th beam.

The standard procedure to assess the natural frequencies and the mode shapes of the i th EB beam is [Craig, 2006]:

- I) Starting from Eq. (34), the boundary conditions at $x_i = 0$ and $x_i = L_i$ are enforced to yield a set of 4 equations which solution provides the expressions of the coefficients $C_{i,p}^{(1)}, C_{i,p}^{(2)}, C_{i,p}^{(3)}, C_{i,p}^{(4)}$.
- II) The non-trivial solution of this system of equations is the so-called characteristic equation and it is a function of $\eta_{i,p}$. This equation is obtained by imposing the vanishing of the coefficient matrix's determinant. The solution of the characteristic equation are the parameters $\eta_{i,p}$. These parameters cannot be found in closed-form since the characteristic equation is a combination of trigonometric and hyperbolic functions. Therefore, $\eta_{i,p}$ are obtained numerically. The natural frequencies can now be obtained as:

$$\omega_{i,p} = \sqrt{\frac{EI_i \eta_{i,p}^4}{\rho_i A_i}} \quad (35)$$

- III) The p th mode shape for each $\eta_{i,p}$ is found by replacing the coefficients $C_{i,p}^{(1)}, C_{i,p}^{(2)}, C_{i,p}^{(3)}, C_{i,p}^{(4)}$ in Eq. (34).
- IV) These mode shapes have to be scaled to yield the so-called normal mode shapes $\bar{\Phi}_{i,p}(x_i)$. The two commonest procedures employed for scaling modes are:
 - 1) Scale the mode such that the maximum value of the amplitude is unitary:

$$\max_{x_i} |\bar{\Phi}_{i,p}(x_i)| = 1 \quad (36)$$

2) Scale the mode such that the generalized mass, or modal mass, $M_{i,p}$ related to the p th mode, assumes unitary value:

$$M_{i,p} = \int_0^{L_i} \rho_i A_i \bar{\Phi}_{i,p}^2 dx = 1 \quad (37)$$

In this paper, the normal mode shapes are normalized employing the second procedure.

V) The following orthogonality proprieties hold:

$$\int_0^{L_i} \rho_i A_i \bar{\Phi}_{i,p}(x) \bar{\Phi}_{i,k}(x) dx = \bar{\delta}_{pk} \quad (38)$$

$$\int_0^{L_i} EI_i \bar{\Phi}_{i,p}''(x) \bar{\Phi}_{i,k}''(x) dx = \omega_{i,p}^2 \bar{\delta}_{pk} \quad (39)$$

where $\bar{\Phi}_{i,p}(x)$ and $\bar{\Phi}_{i,k}(x)$ are two generic mode shapes, and $\bar{\delta}_{pk}$ is the Kronecker's delta function defined as follow:

$$\bar{\delta}_{pk} = \begin{cases} 0 & \text{if } p \neq k \\ 1 & \text{if } p = k \end{cases} \quad (40)$$

Once the normal mode shapes are known, the problem of forced and damped vibrations of the i th EB beam can be tackled.

Eq. (25) can now be written as:

$$\begin{aligned} EI_i \sum_{s=1}^{\infty} \bar{\Phi}_{i,s}''''(x_i) \mathcal{G}_{i,s}(t) + \left[c_{K,i} EI_i \sum_{s=1}^{\infty} \bar{\Phi}_{i,s}''''(x_i) + c_{M,i} \rho_i A_i \sum_{s=1}^{\infty} \bar{\Phi}_{i,s}(x_i) \right] \dot{\mathcal{G}}_{i,s}(t) + \\ + \rho_i A_i \sum_{s=1}^{\infty} \bar{\Phi}_{i,s}(x_i) \ddot{\mathcal{G}}_{i,s}(t) = f_z(x_i, t) \end{aligned} \quad (41)$$

Moreover, from Eq. (31), for the p th mode shapes the following relationship holds:

$$EI_i \bar{\Phi}_{i,p}''''(x_i) = \rho_i A_i \omega_{i,p}^2 \bar{\Phi}_{i,p}(x_i) \quad (42)$$

Therefore, accounting for Eq.(42), Eq. (41) can be written as:

$$\rho_i A_i \sum_{s=1}^{\infty} \bar{\Phi}_{i,s}(x_i) \left[\omega_{i,s}^2 \mathcal{G}_{i,s}(t) + (c_{K,i} \omega_{i,s}^2 + c_{M,i}) \dot{\mathcal{G}}_{i,s}(t) + \ddot{\mathcal{G}}_{i,s}(t) \right] = f_z(x_i, t) \quad (43)$$

Multiplying Eq. (43) by $\bar{\Phi}_{i,p}(x)$ and integrating from 0 to L_i , using the orthogonal conditions (Eqs. (38), (39)), the governing equation of the p th forced-damped single-degree-of-freedom (SDOF) system, is:

$$\ddot{\mathcal{G}}_{i,p}(t) + (c_{K,i} \omega_{i,p}^2 + c_{M,i}) \dot{\mathcal{G}}_{i,p}(t) + \omega_{i,p}^2 \mathcal{G}_{i,p}(t) = F_{i,p}(t) \quad (44)$$

where $F_{i,p}(t)$ is the so-called generalized force corresponding to $\mathcal{G}_{i,p}(t)$, defined as:

$$F_{i,p}(t) = \int_0^{L_i} \bar{\Phi}_{i,p}(x_i) f_z(x_i, t) dx$$

Introducing the modal damping ratio $\zeta_{i,p}$ for the p th mode as [Chopra, 2001]:

$$\zeta_{i,p} = \frac{c_{M,i}}{2} \frac{1}{\omega_{i,p}} + \frac{c_{K,i}}{2} \omega_{i,p} \quad (45)$$

Eq. (44) is written:

$$\ddot{\mathcal{G}}_{i,p}(t) + 2\zeta_{i,p}\omega_{i,p}\dot{\mathcal{G}}_{i,p}(t) + \omega_{i,p}^2 \mathcal{G}_{i,p}(t) = F_{i,p}(t) \quad (46)$$

The Rayleigh damping constants $c_{M,i}$ and $c_{K,i}$ can be determined from specified damping ratios $\zeta_{i,j}$ and $\zeta_{i,k}$ for the j th and k th modes, respectively. For example, assuming $\zeta_{i,j} = \zeta_{i,k} = \zeta$ yields [Chopra, 2001]:

$$c_{M,i} = \zeta \frac{2\omega_{i,j}\omega_{i,k}}{\omega_{i,j} + \omega_{i,k}} \quad (47)$$

$$c_{K,i} = \zeta \frac{2}{\omega_{i,j} + \omega_{i,k}} \quad (48)$$

The solution of Eq. (46) yields the generalised coordinate $\mathcal{G}_{i,p}(t)$ relative to the p th mode.

The response of the i th EB beam obtained with Eq. (26) can be approximated by considering a finite number of normal mode shapes m which are significantly excited by the external load, so that:

$$W_i(x_i, t) \approx \sum_{s=1}^m \bar{\Phi}_{i,s}(x_i) \mathcal{G}_{i,s}(t) \quad (49)$$

This means solving m independent equations of the generalised coordinate (Eq. (46)). The solution of the m SDOF systems (Eq. (46)) can be found via the classical numerical integration techniques (e.g. Newmark-beta method, Wilson-theta method and transition matrix method) [Chopra, 2001].

3.2 Forced vibration analysis of jointed EB damped beam

In this section, the approach is generalised to tackle jointed EB beams, as the one shown in **Figure 3**. The beam is composed of an assembly of $N+1$ EB beams each with flexural stiffness EI_i , density ρ_i and cross-area section A_i , being N the number of discontinuity points. The internal rotational springs (stiffness $k_{r,i}$), internal translational springs (stiffness $k_{t,i}$) and along-axis external translational springs (stiffness $\bar{k}_{t,i}$) at each discontinuity points are taken into account. Moreover, $k_{te,1}, k_{te,2}$, and $k_{re,1}, k_{re,2}$ are respectively the translational and rotational stiffnesses, associated to the boundary conditions of the jointed EB beam.

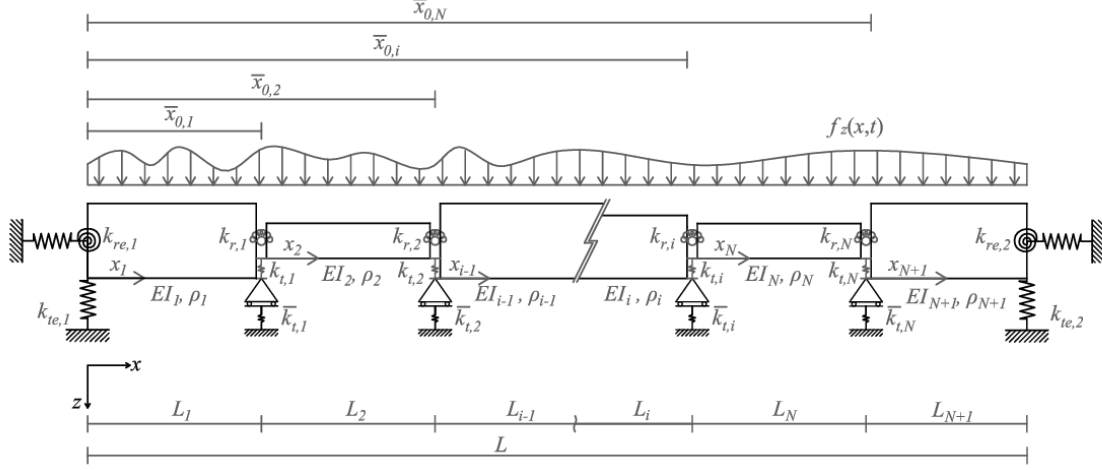


Figure 3 Jointed EB beam with multiple step changes in cross-section, arbitrary boundary conditions, along-axis springs and internal rotational and translational springs at the discontinuities, subjected to an arbitrary dynamic load.

In **Figure 3**, the term $\bar{x}_{0,i}$ indicates the position of the discontinuity of the i th interface, with respect to the global coordinate system. While x_i is the local coordinate system of the i th beam.

The following relationships between the global (x) and local coordinate (x_i) systems hold:

$$x_1 = x; \quad x_2 = x - \bar{x}_{0,1}, \dots, \quad x_i = x - \bar{x}_{0,i-1} \quad (50)$$

Similarly to what suggest by Xu et al [2013] using a different formulation, the local reference system is used here to obtain compact expressions for the undamped free vibration of the i th EB beam, and therefore of the jointed EB beam, and to reduce the numerical instabilities due to the presence of the hyperbolic functions in the evaluation of high order modes.

The case for which no internal or external springs are considered is covered in **Section 3.2.1**, while the presence of them is taken into account in **Section 3.2.2**.

3.2.1 Forced vibration analysis of the jointed EB damped beam with step changes in flexural stiffness, cross section and density

Let us consider a jointed EB damped beam with step changes in flexural stiffness, cross-section and density. Similarly to the static case, the flexural rigidity variation $EI(x)$ can be expressed with the generalized function:

$$EI(x) = EI_1(x) + \sum_{i=2}^{N+1} [EI_i(x - \bar{x}_{0,i-1}) - EI_{i-1}(x - \bar{x}_{0,i-2})] H(x - \bar{x}_{0,i-1}) \quad (51)$$

In the dynamic case, it is also necessary to take into account the cross-section area $A(x)$ and the density $\rho(x)$ variations. Therefore, the generalised functions can be used to yield:

$$A(x) = A_1(x) + \sum_{i=2}^{N+1} [A_i(x - \bar{x}_{0,i-1}) - A_{i-1}(x - \bar{x}_{0,i-2})] H(x - \bar{x}_{0,i-1}) \quad (52)$$

$$\rho(x) = \rho_1(x) + \sum_{i=2}^{N+1} [\rho_i(x - \bar{x}_{0,i-1}) - \rho_{i-1}(x - \bar{x}_{0,i-2})] H(x - \bar{x}_{0,i-1}) \quad (53)$$

where the notation used is such that $\bar{x}_{0,0} = 0$.

As for the static case (Eq. (8)) the time-dependent deflection of the jointed beam can now be written as:

$$W(x, t) = W_1(x, t) + \sum_{i=2}^{N+1} [W_i(x, t) - W_{i-1}(x, t)] H(x - \bar{x}_{0,i-1}) \quad (54)$$

The $W_i(x, t)$ is the time deflection of an equivalent homogenous beam with flexural rigidity EI_i , density ρ_i and cross-section area A_i . Since $W_i(x, t)$ can be expressed as the sum of the product of the mode shapes and the generalized coordinates (Eq. (26)), the Heaviside's unit step function in Eq. (54) will affect only the mode shapes. Therefore, the p th mode shape of the jointed EB beam is expressed as:

$$\hat{\Phi}_p(x) = \hat{\Phi}_{1,p}(x) + \sum_{i=2}^{N+1} [\hat{\Phi}_{i,p}(x - \bar{x}_{0,i-1}) - \hat{\Phi}_{i-1,p}(x - \bar{x}_{0,i-2})] H(x - \bar{x}_{0,i-1}) \quad (55)$$

where $\hat{\Phi}_{i,p}(x_i)$ is the p th mode shape of the i th homogeneous EB beam with flexural rigidity EI_i , density ρ_i and cross-section area A_i as expressed in Eq. (34). Similarly to the static case, the 4 constants and the frequency parameter of the mode shape of each i th beam can be expressed as a function of the preceding beam by explicitly enforcing the continuity conditions at each interface. As a result, the expression in Eq. (55) depends only on 4 constants and on the m frequency parameters (being m the mode number). Moreover, each frequency parameters $\eta_{i,p}$ will be expressed as function of the natural frequencies ω_p of the entire jointed EB beam.

Let us derive first the recursive expression of the 4 constants. By using the generalized functions, the slope ($\hat{\Psi}_{i,p}(x_i) = \hat{\Phi}'_{i,p}(x_i)$), bending moment ($\hat{M}_{i,p}(x_i) = -EI_i \hat{\Phi}''_{i,p}(x_i)$) and shear ($\hat{T}_{i,p}(x_i) = -EI_i \hat{\Phi}'''_{i,p}(x_i)$) functions of the p th mode shape of the whole jointed EB beam can be expressed as:

$$\hat{\Psi}_p(x) = \hat{\Psi}_{1,p}(x_1) + \sum_{i=2}^{N+1} [\hat{\Psi}_{i,p}(x - \bar{x}_{0,i-1}) - \hat{\Psi}_{i-1,p}(x - \bar{x}_{0,i-2})] H(x - \bar{x}_{0,i-1}) \quad (56)$$

$$\hat{M}_p(x) = \hat{M}_{1,p}(x_1) + \sum_{i=2}^{N+1} [\hat{M}_{i,p}(x - \bar{x}_{0,i-1}) - \hat{M}_{i-1,p}(x - \bar{x}_{0,i-2})] H(x - \bar{x}_{0,i-1}) \quad (57)$$

$$\hat{T}_p(x) = \hat{T}_{1,p}(x_1) + \sum_{i=2}^{N+1} [\hat{T}_{i,p}(x - \bar{x}_{0,i-1}) - \hat{T}_{i-1,p}(x - \bar{x}_{0,i-2})] H(x - \bar{x}_{0,i-1}) \quad (58)$$

As for the static case, dimensionless quantities can be introduced to describe the relationships between flexural rigidities, and also cross-area sections and densities of two successive beams:

$$\tilde{\gamma}_i = \frac{EI_{i+1}}{EI_i} \quad (59)$$

$$\tilde{\alpha}_i = \frac{A_{i+1}}{A_i} \quad (60)$$

$$\tilde{\nu}_i = \frac{\rho_{i+1}}{\rho_i} \quad (61)$$

Using the dimensionless coefficients defined in the previous equations, the frequencies parameters of two successive beams can be related such that:

$$\eta_{i+1,p} = \tilde{\beta}_i \eta_{i,p} \quad (62)$$

where $\tilde{\beta}_i$ is a dimensionless coefficient of the i th beam defined as:

$$\tilde{\beta}_i = \sqrt[4]{\frac{\tilde{\alpha}_i \tilde{\nu}_i}{\tilde{\gamma}_i}} \quad (63)$$

Similarly to the static case, these quantities, together with the enforcement of the continuity conditions in terms of the mode shape ($\hat{\Phi}_{i,p}(\bar{x}_{0,i}) = \hat{\Phi}_{i+1,p}(0)$), slope ($\hat{\Psi}_{i,p}(\bar{x}_{0,i}) = \hat{\Psi}_{i+1,p}(0)$), shear force ($\hat{T}_{i,p}(\bar{x}_{0,i}) = \hat{T}_{i+1,p}(0)$) and bending moment ($\hat{M}_{i,p}(\bar{x}_{0,i}) = \hat{M}_{i+1,p}(0)$), enable to reduce the $4N$ unknown coefficients to 4 unknown coefficients which can be found by imposing the 4 boundary conditions only:

$$C_{i+1,p}^{(1)} = \frac{1}{2\eta_{i,p}^3} (\eta_{i,p}^3 C_{i,p}^{(1)} \Gamma_{i,p}^{(1)} + \eta_{i,p}^2 C_{i,p}^{(2)} \Gamma_{i,p}^{(3)} + \eta_{i,p} C_{i,p}^{(3)} \Gamma_{i,p}^{(2)} + C_{i,p}^{(4)} \Gamma_{i,p}^{(4)}) \quad (64)$$

$$C_{i+1,p}^{(2)} = \frac{1}{2\eta_{i,p}^2} (\eta_{i,p}^3 C_{i,p}^{(1)} \Gamma_{i,p}^{(4)} + \eta_{i,p}^2 C_{i,p}^{(2)} \Gamma_{i,p}^{(1)} + \eta_{i,p} C_{i,p}^{(3)} \Gamma_{i,p}^{(3)} + C_{i,p}^{(4)} \Gamma_{i,p}^{(2)}) \quad (65)$$

$$C_{i+1,p}^{(3)} = \frac{1}{2\gamma_i \eta_{i,p}} (\eta_{i,p}^3 C_{i,p}^{(1)} \Gamma_{i,p}^{(2)} + \eta_{i,p}^2 C_{i,p}^{(2)} \Gamma_{i,p}^{(4)} + \eta_{i,p} C_{i,p}^{(3)} \Gamma_{i,p}^{(1)} + C_{i,p}^{(4)} \Gamma_{i,p}^{(3)}) \quad (66)$$

$$C_{i+1,p}^{(4)} = \frac{1}{2\gamma_i} (\eta_{i,p}^3 C_{i,p}^{(1)} \Gamma_{i,p}^{(3)} + \eta_{i,p}^2 C_{i,p}^{(2)} \Gamma_{i,p}^{(2)} + \eta_{i,p} C_{i,p}^{(3)} \Gamma_{i,p}^{(4)} + C_{i,p}^{(4)} \Gamma_{i,p}^{(1)}) \quad (67)$$

where the functions $\Gamma_{i,p}^{(1)}, \Gamma_{i,p}^{(2)}, \Gamma_{i,p}^{(3)}, \Gamma_{i,p}^{(4)}$ are defined as:

$$\Gamma_{i,p}^{(1)} = \cosh(L_i \eta_{i,p}) + \cos(L_i \eta_{i,p}) \quad (68)$$

$$\Gamma_{i,p}^{(2)} = \cosh(L_i \eta_{i,p}) - \cos(L_i \eta_{i,p}) \quad (69)$$

$$\Gamma_{i,p}^{(3)} = \sinh(L_i \eta_{i,p}) + \sin(L_i \eta_{i,p}) \quad (70)$$

$$\Gamma_{i,p}^{(4)} = \sinh(L_i \eta_{i,p}) - \sin(L_i \eta_{i,p}) \quad (71)$$

Similarly to the steps summarized for the i th beam (**Section 3.1**), the procedure to assess the natural frequencies and the mode shapes of the jointed EB beam is:

- I) The expressions of the coefficients $C_{1,p}^{(1)}, C_{1,p}^{(2)}, C_{1,p}^{(3)}, C_{1,p}^{(4)}$ are evaluated by solving a set of 4 equations obtained by enforcing the boundary conditions at $x = 0$ and $x = L$ in terms of Eqs. (55), (56), (57), (58).

- II) The characteristic equation is obtained by imposing the vanishing of the coefficient matrix's determinant of this system of equations. The solutions, $\eta_{l,p}$, of the characteristic equation are obtained numerically, so the natural frequencies can be obtained as:

$$\omega_p = \sqrt{\frac{EI_1 \eta_{l,p}^4}{\rho_1 A_1}} \quad (72)$$

- III) The p th mode shape for each $\eta_{l,p}$ is found by replacing the coefficients $C_{1,p}^{(1)}, C_{1,p}^{(2)}, C_{1,p}^{(3)}, C_{1,p}^{(4)}$ in Eq. (55).
- IV) The normal mode shapes $\bar{\Phi}_p(x)$ are obtained by scaling the modes $\hat{\Phi}_p(x)$ (Eq. (55)) such that the generalized mass, or modal mass, M_p related to the p th mode, assumes unitary value:

$$M_p = \int_0^L \rho(x) A(x) \bar{\Phi}_p^2 dx = 1 \quad (73)$$

where $\rho(x)$ and $A(x)$ are the density and cross-area functions defined in Eq. (53) and Eq. (52), respectively.

- V) The following orthogonality proprieties hold:

$$\int_0^L \rho(x) A(x) \bar{\Phi}_p(x) \bar{\Phi}_k(x) dx = \bar{\delta}_{pk} \quad (74)$$

$$\int_0^L EI(x) \bar{\Phi}_p''(x) \bar{\Phi}_k''(x) dx = \omega_p^2 \bar{\delta}_{pk} \quad (75)$$

where $\bar{\Phi}_p(x)$ and $\bar{\Phi}_k(x)$ are two generic mode shapes, $\bar{\delta}_{pk}$ is the Kronecker's delta function and $EI(x)$ is the flexural rigidity defined in Eq. (51).

Once the normal mode shapes are known, the problem of forced vibrations of the jointed EB damped beam can be tackled, as done for the i th EB beam in **Section 3.1**.

In this case, the governing equation of the p th forced-damped single-degree-of-freedom (SDOF) system (Eq. (46)), becomes:

$$\ddot{\mathcal{G}}_p(t) + 2\zeta_p \omega_p \dot{\mathcal{G}}_p(t) + \omega_p^2 \mathcal{G}_p(t) = F_p(t) \quad (76)$$

where the generalized force $F_p(t)$ corresponding to $\mathcal{G}_p(t)$ is:

$$F_p(t) = \int_0^L \bar{\Phi}_p(x) f_z(x, t) dx \quad (77)$$

while the modal damping ζ_p is:

$$\zeta_p = \frac{c_M}{2} \frac{1}{\omega_p} + \frac{c_K}{2} \omega_p \quad (78)$$

The Rayleigh damping constants c_M and c_K are assessed by accounting for two modes of the jointed EB beam as explained in **Section 3.1** for the i th EB beam.

It is worth noting that the dynamic transversal load $f_z(x, t)$ can be expressed with the generalised functions, so that for example a sinusoidal point force of amplitude F_0 , frequency ω_F applied at abscissa x_F can be expressed as $f_z(x, t) = F_0 \delta(x - x_F) \sin(\omega_F t)$. By replacing $f_z(x, t)$ in Eq. (77) it is clear that the Dirac's delta affects the mode shape contribution only. Similarly to what was described in **Section 3.1**, the response of the jointed EB beam in terms of displacement $W(x, t)$ can be approximated by using a finite number of normal mode shapes m :

$$W(x, t) \approx \sum_{s=1}^m \bar{\Phi}_s(x) \mathcal{G}_s(t) \quad (79)$$

3.2.2 Forced vibration analysis of the jointed EB damped beam with step changes in flexural stiffness, cross-section and density with internal and/or external springs at the interface points

Let us consider a jointed EB damped beam with step changes in flexural stiffness, cross-section and density with rotational and/or translational internal springs and/or external translational springs at the interface points.

The procedure explained in **Section 3.2.1** need to be particularized to include the presence of internal translational, internal rotational and along-axis springs which cause unknowns variations of $\hat{\Phi}_p(\bar{x}_{0,i})$, $\hat{\Psi}_p(\bar{x}_{0,i})$ and $\hat{T}_p(\bar{x}_{0,i})$ at the interface points. These unknown variations can be expressed as $\Delta\phi_{i,p}$, $\Delta\psi_{i,p}$ and $\Delta T_{i,p}$. The coefficients $C_{1,p}^{(1)}$, $C_{1,p}^{(2)}$, $C_{1,p}^{(3)}$, $C_{1,p}^{(4)}$, $\Delta\phi_{i,p}$, $\Delta\psi_{i,p}$, $\Delta T_{i,p}$ are evaluated by imposing the 4 boundary conditions together with one continuity condition for each spring.

The internal rotational springs (stiffness $k_{r,i}$), internal translational springs (stiffness $k_{t,i}$) and along-axis external translational springs (stiffness $\bar{k}_{t,i}$) at the discontinuity interfaces can be expressed as:

$$\hat{M}_p(\bar{x}_{0,i}) = k_{r,i} \Delta\psi_{i,p} \quad (80)$$

$$\hat{T}_p(\bar{x}_{0,i}) = k_{t,i} \Delta\phi_{i,p} \quad (81)$$

$$\hat{\Phi}_p(\bar{x}_{0,i}) = -\frac{\Delta T_{i,p}}{\bar{k}_{t,i}} \quad (82)$$

The continuity conditions at the interfaces can be expressed in terms of mode shape ($\hat{\Phi}_{i,p}(\bar{x}_{0,i}) + \Delta\phi_{i,p} = \hat{\Phi}_{i+1,p}(0)$), slope ($\hat{\Psi}_{i,p}(\bar{x}_{0,i}) + \Delta\psi_{i,p} = \hat{\Psi}_{i+1,p}(0)$), shear force ($\hat{T}_{i,p}(\bar{x}_{0,i}) + \Delta T_{i,p} = \hat{T}_{i+1,p}(0)$) and bending moment ($\hat{M}_{i,p}(\bar{x}_{0,i}) = \hat{M}_{i+1,p}(0)$).

The constants expressions can now be found as:

$$C_{i+1,p}^{(1)} = \frac{1}{2\eta_{i,p}^3} (\eta_{i,p}^3 C_{i,p}^{(1)} \Gamma_{i,p}^{(1)} + \eta_{i,p}^2 C_{i,p}^{(2)} \Gamma_{i,p}^{(3)} + \eta_{i,p} C_{i,p}^{(3)} \Gamma_{i,p}^{(2)} + C_{i,p}^{(4)} \Gamma_{i,p}^{(4)}) + \Delta\phi_{i,p} \quad (83)$$

$$C_{i+1,p}^{(2)} = \frac{1}{2\eta_{i,p}^2} \left(\eta_{i,p}^3 C_{i,p}^{(1)} \Gamma_{i,p}^{(4)} + \eta_{i,p}^2 C_{i,p}^{(2)} \Gamma_{i,p}^{(1)} + \eta_{i,p} C_{i,p}^{(3)} \Gamma_{i,p}^{(3)} + C_{i,p}^{(4)} \Gamma_{i,p}^{(2)} \right) + \Delta \psi_{i,p} \quad (84)$$

$$C_{i+1,p}^{(3)} = \frac{1}{2\gamma_i \eta_{i,p}} \left(\eta_{i,p}^3 C_{i,p}^{(1)} \Gamma_{i,p}^{(2)} + \eta_{i,p}^2 C_{i,p}^{(2)} \Gamma_{i,p}^{(4)} + \eta_{i,p} C_{i,p}^{(3)} \Gamma_{i,p}^{(1)} + C_{i,p}^{(4)} \Gamma_{i,p}^{(3)} \right) \quad (85)$$

$$C_{i+1,p}^{(4)} = \frac{1}{2\gamma_i} \left(\eta_{i,p}^3 C_{i,p}^{(1)} \Gamma_{i,p}^{(3)} + \eta_{i,p}^2 C_{i,p}^{(2)} \Gamma_{i,p}^{(2)} + \eta_{i,p} C_{i,p}^{(3)} \Gamma_{i,p}^{(4)} + C_{i,p}^{(4)} \Gamma_{i,p}^{(1)} \right) + \frac{\Delta T_{i,p}}{\gamma_i EI_i} \quad (86)$$

where the functions $\Gamma_{i,p}^{(1)}$, $\Gamma_{i,p}^{(2)}$, $\Gamma_{i,p}^{(3)}$, $\Gamma_{i,p}^{(4)}$ have already been defined in Eqs. (68), (69), (70), (71), respectively.

It can be noted that Eq. (85) is unchanged from Eq. (66) while the other expressions are characterized by an additional term related to the local variations. In a similar fashion, other types of discontinuities can be treated, introducing additional terms to the expressions of the constants.

In conclusion, the proposed approach yields a single equation describing the mode shapes of jointed EB beams with step changes in flexural stiffness, cross-section and density with rotational, translational internal springs and external translational springs at the interface points which depends only on 4 constants on the m frequency parameter (being m the mode number). Closed-form expressions for the constants are provided. These expressions include also the additional variations produced by each internal or external spring at the interfaces. The mode shape expression is used to evaluate the characteristic function, and consequently each natural frequency and the corresponding mode shape. It is worth noting that, similarly to the static case, for r unknown variations at the interfaces, the system of equations that need to be solved is of $4+r$ equations, being 4 the number of boundary conditions. By taking into account a local reference system, numerical instabilities due to the presence of the hyperbolic functions in the evaluation of high order modes are reduced, as shown in the following numerical applications. Having determined the mode shapes, these can be readily used to evaluate the forced response. The proposed method is therefore an efficient alternative to the approach proposed by Lin and Ng [2017] using the elemental impedance method, it does not require a lumped-mass approximation (which was employed in Failla and Santini [2008]) and compared to Torabi et al. [2013] and Xu et al [2013], it can easily account for non-ideal joints.

4. Numerical application

Two numerical applications are presented in this section to validate the proposed approach for the static and dynamic analyses of jointed EB beams.

4.1 Static response of a jointed Euler-Bernoulli beam

The jointed beam depicted in **Figure 4** is an assembly of four distinct EB beams linked in the three discontinuity points $\bar{x}_{0,1} = 1.25$ m, $\bar{x}_{0,2} = 2.50$ m and $\bar{x}_{0,3} = 3.75$ m, and the following translational and rotational springs parameters are considered: $\bar{k}_{t,1} = \bar{k}_{t,3} = 214752$ kN/m, $k_{te,2} = 107377$ kN/m, $k_{r,2} = 270$ kNm and $k_{r,2} = 150$ kN/m.

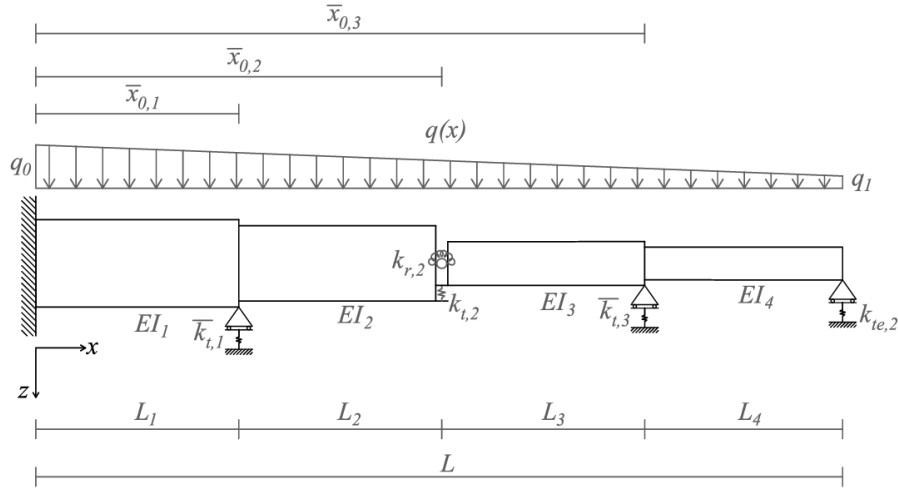


Figure 4 Jointed EB beam with four flexural rigidity discontinuities and various boundary conditions subjected to a trapezoidal static load.

The four linked beams are characterized by rectangular sections, the mechanical and geometrical characteristics are reported in **Table 1**.

Beam	Material	Length [m]	Young's modulus [kN/m ²]	Width [m]	Height [m]	Second moment of area [m ⁴]	Flexural rigidity [kNm ²]
1	Concrete C28/30	1.25	3.2308×10^7	0.30	0.80	0.01280	413542
2	Concrete C25/30	1.25	3.1476×10^7	0.30	0.60	0.00540	169970
3	Concrete C25/30	1.25	3.1476×10^7	0.30	0.40	0.00160	50361.60
4	Concrete C25/30	1.25	3.1476×10^7	0.30	0.30	0.000675	21246.30

Table 1 Geometrical and mechanical characteristics of the jointed EB beam depicted in **Figure 4**.

The beam is subject to a trapezoidal load function with $q_0 = 3.00 \text{ kN/m}$ and $q_1 = 2.00 \text{ kN/m}$. The aim of the analysis is to evaluate the beam deflection under the specified static load. The closed-form solution for the static analysis of jointed EB beams proposed in **Section 2** is used here to tackle this problem.

The dimensionless coefficients $\tilde{\gamma}_i$ defined in Eq. (10) take the values summarized in **Table 2**.

Discontinuity (i)	$\tilde{\gamma}_i$
1	0.4110
2	0.2963
3	0.4219

Table 2 Values of the dimensionless coefficients related to the number of discontinuities.

As specified in Eq. (21), the load function can be written to account for the discontinuities, so that:

$$q(x) = \frac{q_1 - q_0}{L}x + q_0 + \Delta T_1 \delta(x - \bar{x}_{0,1}) + \Delta T_3 \delta(x - \bar{x}_{0,3}) + EI_2 \Delta \psi_2 \delta''(x - \bar{x}_{0,2}) + EI_2 \Delta w_2 \delta'''(x - \bar{x}_{0,2}) \quad (87)$$

where ΔT_1 and ΔT_3 are respectively the variation in the shear function at the discontinuity points $\bar{x}_{0,1}$ and $\bar{x}_{0,3}$ due to the reactions forces of the external supports, while $\Delta \psi_2$ and Δw_2 are respectively the variation in the slope function and in the deflection at the discontinuity point $\bar{x}_{0,2}$ due to the presence of an internal rotational and translational spring.

It worth remarking that the values of ΔT_1 , ΔT_3 , $\Delta \psi_2$ and Δw_2 are unknowns. In order to find their value, in addition to the classical four boundary conditions, other four conditions (one for each unknown) have to be taken into account. Therefore, the following system of equations have to be enforced:

$$W(0) = 0 \quad (88)$$

$$\Psi(0) = 0 \quad (89)$$

$$M(L) = 0 \quad (90)$$

$$W(L) = -\frac{T(L)}{k_{te,2}} \quad (91)$$

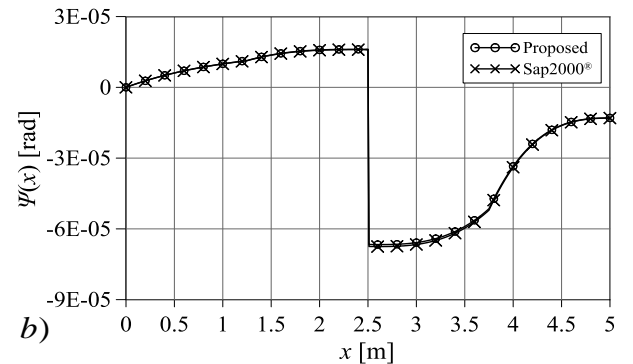
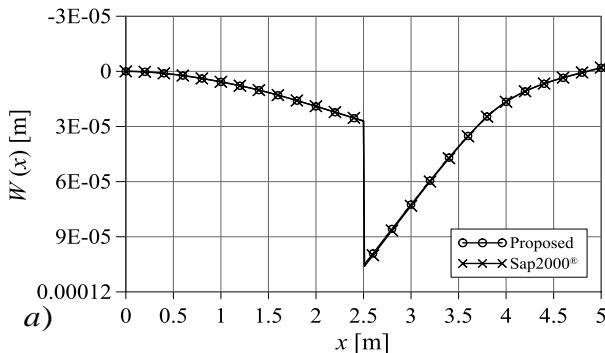
$$W(\bar{x}_{0,1}) = -\frac{\Delta T_1}{\bar{k}_{t,1}} \quad (92)$$

$$M(\bar{x}_{0,2}) = k_{r,2} \Delta \psi_2 \quad (93)$$

$$T(\bar{x}_{0,2}) = k_{t,2} \Delta w_2 \quad (94)$$

$$W(\bar{x}_{0,3}) = -\frac{\Delta T_3}{\bar{k}_{t,3}} \quad (95)$$

The solutions in terms of deflection (**Figure 5a**), slope (**Figure 5b**), shear force (**Figure 5c**) and bending moment (**Figure 5d**), provided by the proposed approach (**Section 2**) are compared with the solutions given by Sap2000®. **Figure 5** shows the results given by the proposed method are perfectly agreement with ones given by the software. Moreover, **Figure 5a**, **Figure 5b** and **Figure 5c** show that the proposed method catches the expected discontinuity in the deflection (due to the internal translational spring), in the slope function (due to the internal hinge) and in the shear function (due to the presence of the intermediate supports), respectively.



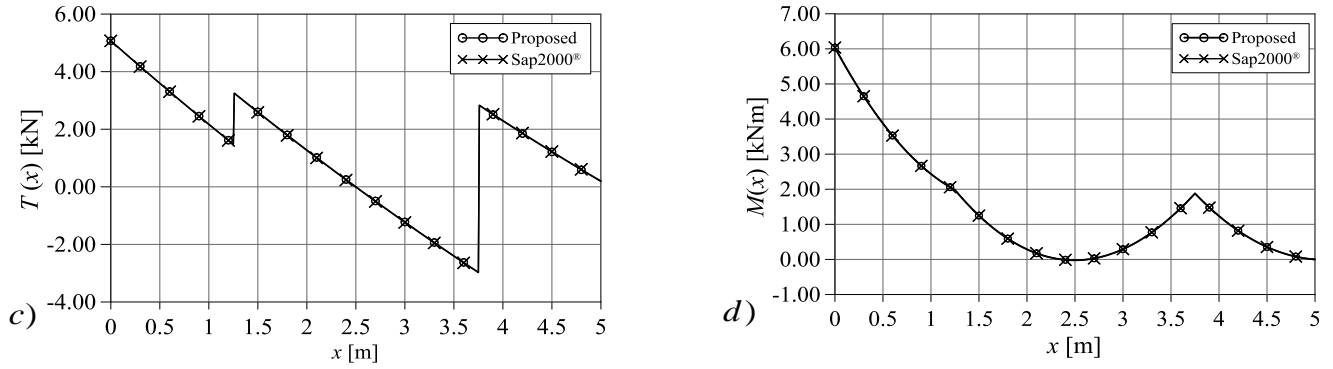


Figure 5 Results obtained with the proposed method and Sap2000® in terms of: a) displacement, b) slope, c) shear force, and d) bending moment.

4.2 Forced-damped vibrations of a jointed Euler-Bernoulli beam

The jointed beam depicted in **Figure 6** is an assembly of three EB beams with circular sections, linked at the two discontinuity points $\bar{x}_{0,1} = 0.80$ m and $\bar{x}_{0,2} = 1.60$ m, respectively.

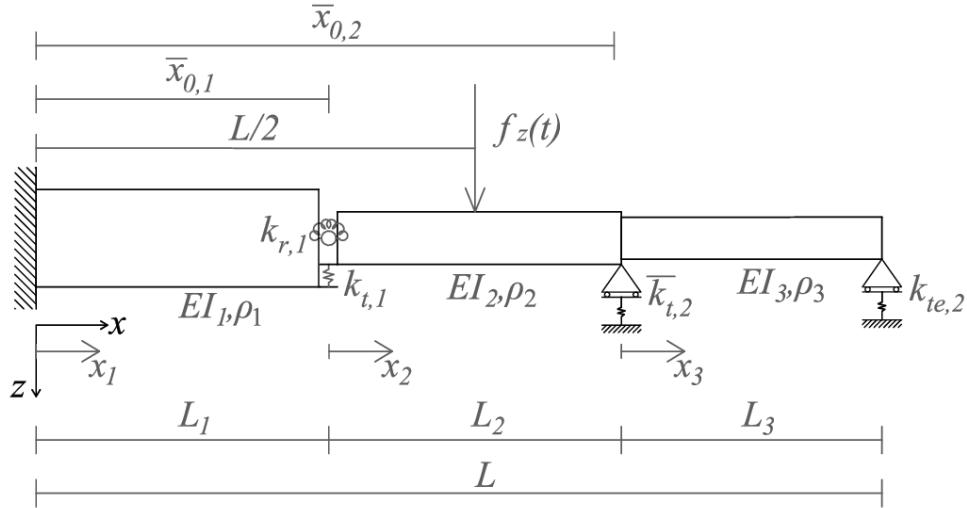


Figure 6 Jointed EB beam with three flexural rigidity discontinuities, various boundary and joints conditions subjected to the dynamic force.

The mechanical and geometrical characteristics of the three jointed beams are summarized in **Table 3**.

Beam	Material	Young's modulus [kN/m ²]	Density [kg/m ³]	Length [m]	Diameter [m]	Area [m ²]	Second moment of area [m ⁴]	Flexural rigidity [kNm ²]
1	steel	2.10×10^8	7800	0.80	0.03	7.06×10^{-4}	3.97×10^{-8}	8349.76
2	aluminium	7.31×10^7	2800	0.80	0.02	3.14×10^{-4}	7.85×10^{-9}	574.13
3	aluminium	7.31×10^7	2800	0.80	0.01	7.85×10^{-5}	4.90×10^{-10}	35.89

Table 3 Geometrical and mechanical characteristics of the jointed EB beam depicted in **Figure 6**.

As shown in **Figure 6**, an internal translational spring ($k_{t,1} = 500$ kN/m) and an internal rotational spring ($k_{r,1} = 270$ kNm) are located at the first interface, while at the second interface

there is an external translational spring ($\bar{k}_{t,2} = 107377$ kN/m). The external support at the end of the jointed beam has translational stiffness $k_{te,2} = 107377$ kN/m.

The dimensionless coefficients defined in Eqs. (59), (60), (61) (63) take the values summarized in **Table 4**.

Discontinuity (i)	$\tilde{\gamma}_i$	$\tilde{\alpha}_i$	$\tilde{\nu}_i$	$\tilde{\beta}_i$
1	6.88×10^{-2}	4.44×10^{-1}	3.58×10^{-1}	1.5945
2	6.25×10^{-2}	2.50×10^{-2}	1	1.41421

Table 4 Values of the dimensionless coefficients related to the number of discontinuities.

The mode shapes of the beam are first evaluated, and then used for the forced analysis considering a low-frequency excitation and a high-frequency excitation.

4.2.1 Mode shapes analysis

The natural frequencies and the corresponding mode shapes of the jointed beam can be computed by using for example the classic approach. With this approach the solution of the jointed beam is obtained by writing the solution for each beam segment using a global coordinate system, and by enforcing the boundary and continuity conditions. Alternatively, the generalised functions can be employed to express the response in a more compact form but still using a global coordinate system. The application of the global coordinate system would significantly limit the number of mode shapes which can be computed accurately. For example, even considering a simplified version of the jointed EB beam in **Figure 6**, with perfect joints, uniform mass density and only step-changes in cross sections, only the first three mode shapes can be computed accurately. Since the numerical instabilities increase when internal constraints and the variability of the mass density are taken into account, using a global coordinate system, for the jointed beam in **Figure 6** would yield less accurate results for the first three modes. Alternatively, the mode shapes can be found by following the procedure explained in **Section 3.2** which uses a local reference system and the generalised functions to yield a closed-form expression of the mode shapes. For the case depicted in **Figure 6**, the constants appearing in this closed-form expression can be found by enforcing the following set of equations:

$$\Phi(0) = 0 \quad (96)$$

$$\Psi(0) = 0 \quad (97)$$

$$M(L) = 0 \quad (98)$$

$$W(L) = -\frac{T(L)}{k_{te,3}} \quad (99)$$

$$T(\bar{x}_{0,1}) = k_{t,1} \Delta \phi_1 \quad (100)$$

$$M(\bar{x}_{0,1}) = k_{r,1} \Delta \psi_1 \quad (101)$$

$$W(\bar{x}_{0,2}) = -\frac{\Delta T_2}{k_{t,2}} \quad (102)$$

In particular, with the proposed approach accurate results for the first nine natural frequencies of the jointed EB beam depicted in **Figure 6** can be obtained. These results are compared to those yielded by Sap2000[®], as reported in **Table 5**, together with the percentage error

$$\varepsilon(\%) = \left(\frac{\omega_{\text{Sap2000}} - \omega_{\text{proposed}}}{\omega_{\text{Sap2000}}} \right) \times 100 \quad (103)$$

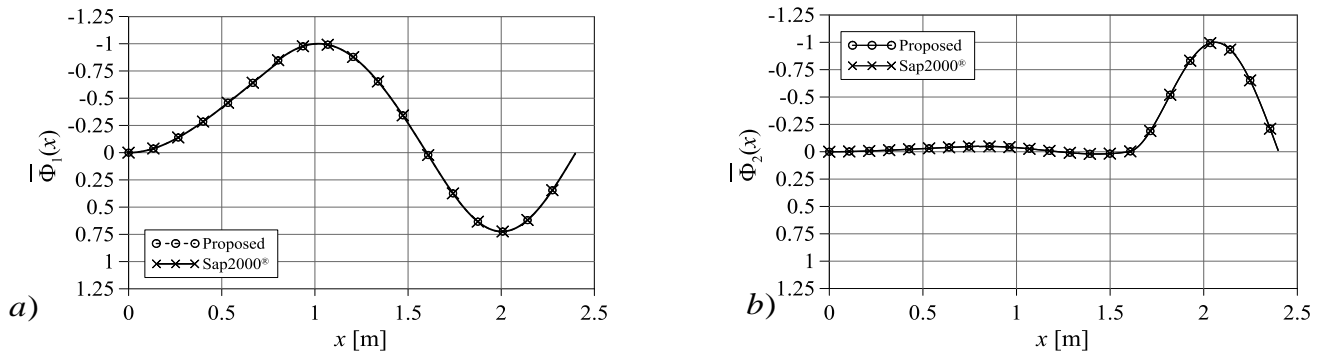
where ω_{Sap2000} is the frequency yielded by Sap2000[®], while ω_{proposed} , is the one obtained with the proposed method.

Mode shape	Natural frequency proposed method (rad/s)	Natural frequency Sap2000 [®] (rad/s)	Percentage error
1	202.49	202.44	-0.0272
2	301.41	301.36	-0.0163
3	602.43	600.67	-0.2928
4	983.20	983.10	-0.0096
5	1265.50	1265.96	0.0364
6	1809.36	1805.40	-0.2193
7	2070.55	2070.27	-0.0139
8	2853.01	2862.14	0.3188
9	3543.00	3541.80	-0.0337

Table 5 Natural frequencies of the jointed EB beam obtained with the proposed method and Sap2000[®], and percentage error.

As the percentage errors in **Table 5** shown, the natural frequencies obtained with the proposed method and the ones yielded by Sap2000[®] are in very good agreement. Sap2000[®] uses the finite element approach, which provides approximated values of natural frequencies even if a dense mesh is considered. This is believed to be the reason for the small differences in the results shown in **Table 5**.

The nine normal mode shapes of the jointed beam obtained with the proposed method and Sap2000[®] are compared in **Figure 7**, where the mode shapes have been scaled with respect to their peak such that the maximum value of their amplitude is unitary. A perfect agreement can be observed. Moreover, the proposed method captures the expected discontinuities. For example, **Figure c**, **Figure 7e**, **Figure 7f**, **Figure 7g**, **Figure 7h** and **Figure 7i** show how the mode shape captures the discontinuities due to the presence of an internal translational spring.



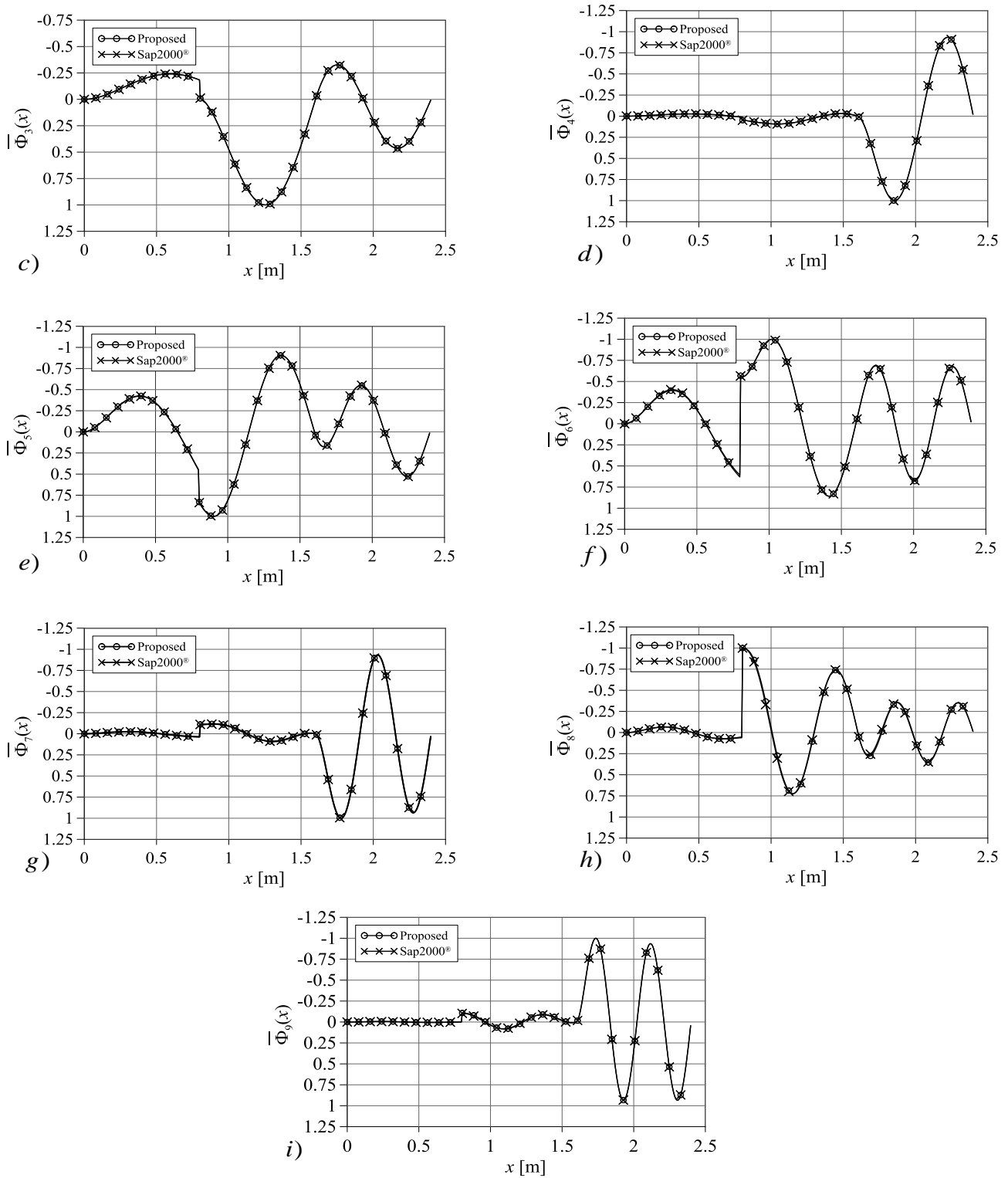


Figure 7 First nine mode shapes of the jointed EB beam obtained with the proposed method and Sap2000®.

The number of modes to be included in the modal expansion depends on the loading acting on the beam. In what follows, this number is chosen by considering the modes appearing in a frequency range that is 10 times bigger than the driving frequency. Low-frequency and a high-frequency excitations are considered and the procedure presented in **Section 3.2** is used to solve the free-undamped and the forced-damped vibrations.

4.2.2 Low-frequency excitation

The jointed beam is subjected to the dynamic force $f_z(x, t)$ defined as:

$$f_z(x, t) = \begin{cases} f_0 \sin(\omega_f t) \delta(x - \tilde{x}) & 0 \leq t \leq 4.8 \text{ s} \\ 0 & 4.8 \leq t \leq 6.0 \text{ s} \end{cases} \quad (104)$$

where, the amplitude $f_0 = 0.050 \text{ kN}$, the driving frequency $\omega_f = 31.4159 \text{ rad/sec}$ and the force is located at $\tilde{x} = 1.20 \text{ m}$. The dynamic load acts for 4.80 seconds ($t_f = 4.8 \text{ s}$), and then the beam experiences free vibration until 6 seconds. The dynamic load used is shown in **Figure 8**.

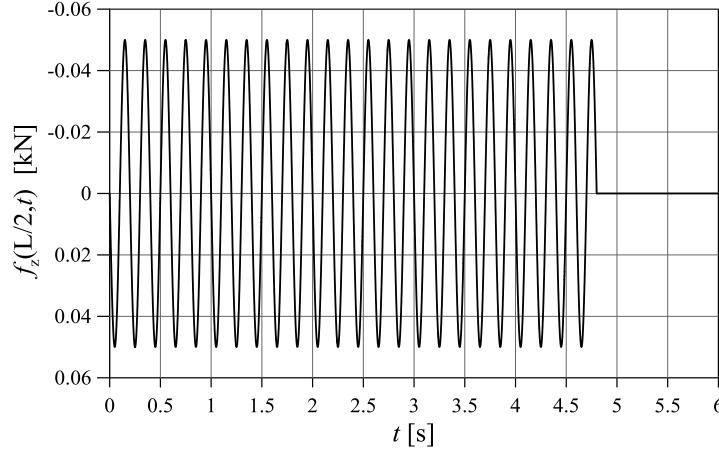


Figure 8 Dynamic force at abscissa $x = L/2$

Given the driving frequency of the loading, only four mode shapes are used to assess the forced-damped vibrations of the jointed beam. These four modes have been scaled such that Eq. (73) holds true. The forced-damped vibrations have been assessed by using the modal analysis approach, considering nine mode shapes, combined with the standard transition matrix method for zero initial conditions ($W(x, t=0)=0$, $\dot{W}(x, t=0)=0$). The Rayleigh damping constants, c_M and c_K , in Eqs. (47), (48) have been considered as $c_M = 4.84482 \text{ s}$ and $c_K = 7.938 \times 10^{-5} \text{ s}^{-1}$, respectively, such that the modal damping ratio for both the first and second mode shape is $\zeta = 0.02$.

Figure 9 shows the response computed at $x = L/2$. In particular, two phases of the response are shown: the forced-damped vibrations up to 4.8 seconds, and the consequent free-damped vibrations up to 6 seconds. The results provided by the proposed method considering four mode shapes are compared with those yielded by Sap2000® considering nine mode shapes, showing a perfect agreement.

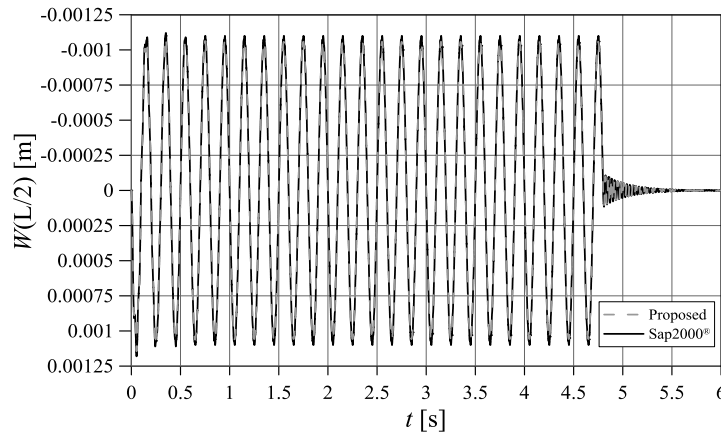


Figure 9 Jointed EB beam response obtained with the proposed method (considering four mode shapes) and with Sap2000® (considering nine mode shapes) at section $x = L/2$ for a driving frequency $\omega_f = 31.4159$ rad/sec.

4.2.3 High-frequency excitation

If an excitation force with driving frequency $\omega_f = 209.44$ rad/sec (33.33 Hz) is considered, nine modes need to be included in the analysis. The response computed at $x = L/2$ with the proposed approach is compared to that yielded by Sap2000® in **Figure 10**.

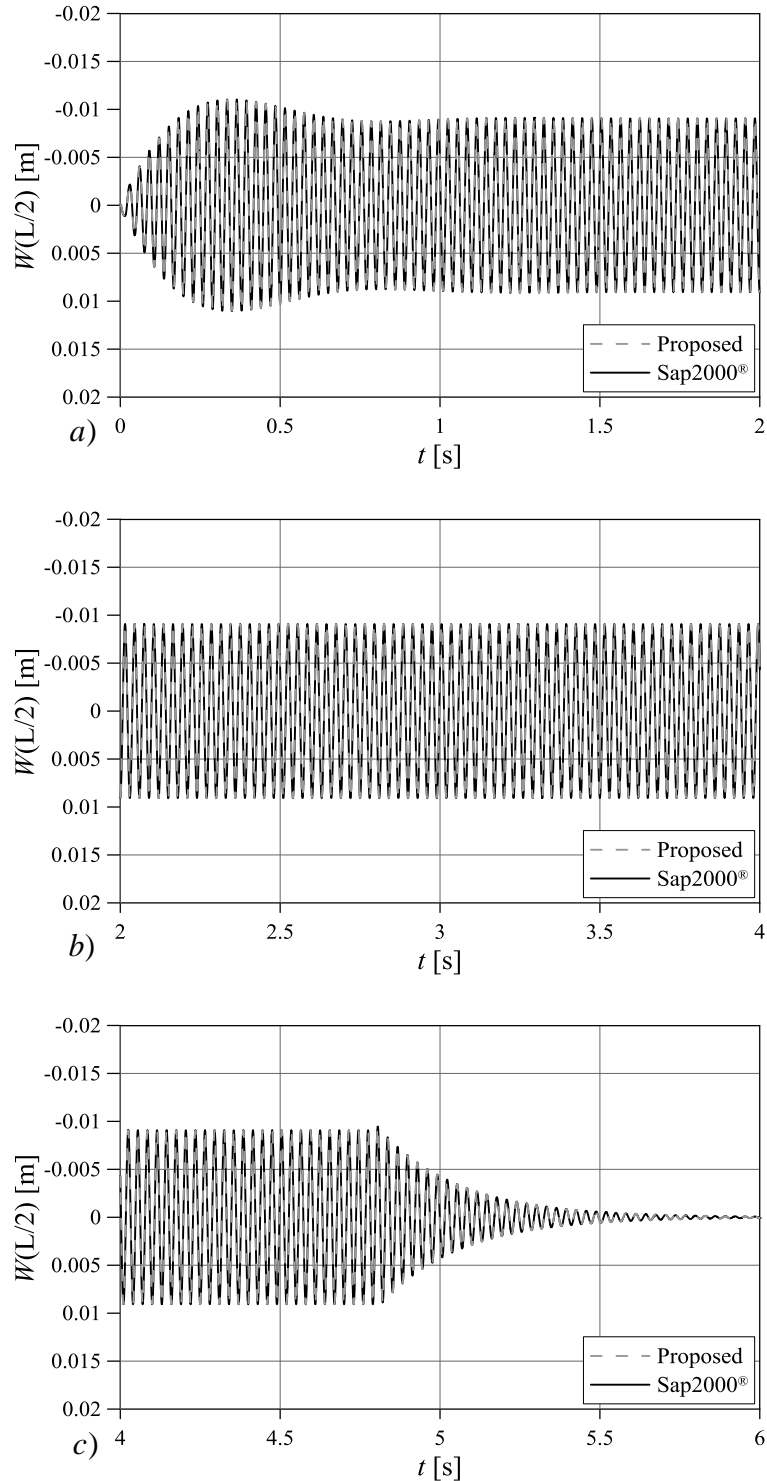


Figure 10 Jointed EB beam response obtained with the proposed method (considering nine mode shapes) and with Sap2000® (considering twelve mode shapes) at section $x = L/2$ for a driving frequency $\omega_f = 209.44$ rad/sec. For visualisation purposes, the response is subdivided into three parts (labelled a), b) and c)) of two seconds each.

From **Figure 10** it is possible to observe that the different phases of the response (forced-damped vibrations up to 4.8 seconds, and the consequent free-damped vibrations up to 6 seconds) are perfectly captured with the proposed approach.

Conclusion

An approach for the static and dynamic analysis of jointed Euler-Bernoulli beams with step changes in material and cross-sections with general boundary conditions, internal rotational, internal translational and external translational springs at the interfaces has been proposed in this paper. Through the proposed approach the jointed Euler-Bernoulli (EB) beam is considered as an assembly of n piecewise homogenous EB beams jointed at their edges. The generalized functions are used to obtain a single expression of static deflection, as well as the mode shapes, which depends on the 4 integration constants associated with the boundary conditions. Closed-form expressions of the 4 constants have been provided. Moreover, in the presence of internal or external springs, one additional constant for each discontinuity has to be taken into account and computed by enforcing one additional equation. Numerical applications regarding the static and dynamic analysis of jointed EB beams with step changes in material and cross-sections with general boundary conditions, internal rotational, internal translational and external translational springs at the interfaces have been presented. The results obtained with the proposed approach have been validated with the commercial finite element software Sap2000®, showing excellent agreement. It is worth remarking that the proposed approach is computationally more efficient than Finite Element procedures, since it yields closed-form solutions that can be readily used for exploring the performance of different designs without remeshing.

Acknowledgements

FG gratefully acknowledge the financial support provided by “Borsa Regionale di Dottorato di Ricerca in Sicilia” [Prot N. 44014] for sponsoring a visiting research stay at the Engineering Science Department of Oxford University. AC is grateful to Balliol College for the Career Development Fellowship in Engineering.

REFERENCES

- [1] Craig Jr R R, Kurdila A J. Fundamentals of Structural Dynamics. 2nd ed. New Jersey: Wiley; 2006.
- [2] Chopra A K. Dynamics of Structures Theory and Applications to Earthquake Engineering. 4th ed. Upper Saddle River: Prentice Hall; 2001.
- [3] Yavari A, Sarkani S. On applications of generalised functions to the analysis of Euler-Bernoulli beam-columns with jump discontinuities. International Journal of Mechanical Sciences Ed. 2001; 43:15432-1562.

- [4] Yavari A, Sarkani S, Moyer E T Jr. On applications of generalised functions to the beam bending problems. *International Journal of Solids and Structures* Ed. 2000; 37:5675-5705.
- [5] Yavari A, Sarkani S, Reddy J N. On nonuniform Euler-Bernoulli and Timoshenko beams with jump discontinuities: application of distribution theory. *International Journal of Solids and Structures* Ed. 2001; 38:8389-8406.
- [6] Biondi B, Caddemi S. Closed-form solutions of Euler-Bernoulli beams with singularities. *International Journal of Solids and Structures* Ed. 2005; 42:3027-3044.
- [7] Biondi B, Caddemi S. Euler-Bernoulli beams with multiple singularities in the flexural stiffness. *European Journal of Mechanics A/Solids* Ed. 2007; 26:789-809.
- [8] Koplow M A, Bhattacharyya A, Mann B P. Closed form solutions for the dynamic response of Euler-Bernoulli beams with step changes in cross-sections. *Journal of Sound and Vibration* Ed. 2006; 295:214-225.
- [9] Stanton S C, Mann B P. On the dynamic response of beams with multiple geometric or material discontinuities. *Mechanical Systems and Signal Processing* Ed. 2010; 24:1409-1419.
- [10] Failla G, Santini A. A solution of Euler-Bernoulli vibrating discontinuous beams. *Mechanics Research Communications* Ed. 2008; 35:517-529.
- [11] Torabi K, Afshari H, Najafi H. Vibration Analysis of Multi-Step Bernoulli-Euler and Timoshenko Beams Carrying Concentrated Masses. *Journal of Solid and Mechanics* Ed. 2013; 5:336-349.
- [12] Gonçalves P J P, Brennan M J, Elliot S J. Numerical evaluation of high-order modes of vibration in uniform Euler-Bernoulli beams. *Journal of Sound and Vibrations* Ed. 2007; 301:1035-1039.
- [13] Xu W, Cao M S, Ren Q, Su Z. Numerical Evaluation of High-Order Modes for Stepped Beam. *Journal of Vibration and Acoustics* Ed. 2013; 136:89-102.
- [14] Lin R M, Ng T Y. Exact vibration modes of multiple-stepped beams with arbitrary steps and supports using elemental impedance method. *Engineering Structures* Ed. 2017; 152:24-34.
- [15] SAP2000, 2009. CSI: Computers and Structures, Inc., Version 14.1.0. Computer software.